



Major Bifurcations, Slip Rates, and A Creeping Segment of Sumatran Fault Zone in Tarutung-Sarulla-Sipirok-Padangsidempuan, Central Sumatra, Indonesia

DANNY HILMAN NATAWIDJAJA

Puslit Geoteknologi - LIPI,
Jln. Sangkuriang, Bandung

Corresponding author: danny.hilman@gmail.com

Manuscript received: January 2, 2018; revised: March 19, 2018;
approved: April 20, 2018; available online: July 20, 2018

Abstract - A detailed active fault study in Tarutung-Sarulla-Sipirok-Padangsidempuan was conducted based on their tectonic-morphological features using SRTM-30, 3D-visualization, and LIDAR data, combined with field and shallow geophysical surveys using the GPR method. Sumatran Fault Zone is bifurcated from the single major Sianok fault segment into two major branches: Angkola and Barumun-Toru Faults that run (sub) parallel to each other. In the studied area, they are merged gradually to become the Renun Fault. The total slip rates from Sianok to Renun segments are constant at about ~ 14 mm/year (13.8 ± 0.3 mm/yr on Renun and 13.7 ± 1.6 mm/yr on Sianok segments). In the bifurcation zone, it is partitioned into 9.3 ± 1.8 mm/yr slip on Toru, and about 4 - 5 mm/yr on Angkola segments. Based on field evidence supported by the seismicity and historical record, the Toru Fault appears to move continuously (creeping). This is crucial for understanding tectonics and its significance to hazard mitigations. Further investigations on Angkola and Toru Faults are crucial for mega installations of Sarulla Geothermal Power Plant, which is located in between Angkola and Toru Fault zones.

Keywords: active faults, Sumatra fault zones, slip rates, fault creeping, seismic hazards, Sarulla geothermal, ground penetration radar, remote sensing

© IJOG - 2018. All right reserved

How to cite this article:

Natawidjaja, D.H., 2018. Major Bifurcations, Slip Rates, and A Creeping Segment of Sumatran Fault Zone in Tarutung-Sarulla-Sipirok-Padangsidempuan, Central Sumatra, Indonesia. *Indonesian Journal on Geoscience*, 5 (2), p.137-160. DOI: [10.17014/ijog.5.2.137-160](https://doi.org/10.17014/ijog.5.2.137-160)

INTRODUCTION

Regional Tectonic

Convergence along Sumatra is highly oblique where tectonic strain is strongly partitioned into a dip-slip on the subduction interface or the megathrust and a dextral slip component on the Sumatran Fault Zone that bisect the Sumatra Island (Fitch, 1972; McCaffrey, 1991; Sieh and Natawidjaja, 2000). With this high relative plate motions and all active fault arrays accomodating the movements, Sumatra rank is considered as

one of the most active seismic region on Earth (Natawidjaja, 2003, 2005, 2012; Natawidjaja *et al.*, 2004; Natawidjaja *et al.*, 2006; Natawidjaja *et al.*, 2007a; ; Natawidjaja *et al.*, 2007b).

Dozens of major destructive earthquakes have occurred in both the megathrust and Sumatran Fault Zone system in the past two centuries. Following the 2004 Aceh-Andaman tsunami-earthquake, seismic activities in Sumatra are unusually hightened, both on the megathrust and along the Sumatran Fault Zone (Nalbant *et al.*, 2006; Sieh *et al.*, 2008).

Sumatran Fault Zone (SFZ) and Purpose of Study

The 1900-km long Sumatran Fault Zone (SFZ) traverses the back-bone of Sumatra within or near the active volcanic arc (Bellier *et al.*, 1997; Katili and Hehuwat, 1967; Natawidjaja *et al.*, 2001; Sieh and Natawidjaja, 2000). The substantial portion of the dextral component of the Sumatran oblique convergence is accommodated by SFZ. At its northern terminus, the SFZ transforms into the spreading centres of the Andaman Sea (Curry, 2005; Curry *et al.*, 1979). At its southern end, around the Sunda Strait, the fault curves southward toward and possibly intersect the Sunda Trench (Diament *et al.*, 1992; Huchon and Pichon, 1984; Sieh and Natawidjaja, 2000) (Figure 1). Sieh and Natawidjaja (2000) mapped the Sumatran Fault Zone using mostly the 1:100,000-scale aerial photographs and the 1:50,000-scale topographic maps. The results of their works are digitized and put into a GIS database. Sumatran fault map created by Sieh and Natawidjaja (2000) has a large-enough scale to enable discrimination

of fault segmentations. Thus, it can be used for a seismic hazard evaluation. The SFZ is highly segmented, and composed of twenty major geometrically defined segments, which vary in length from about 35 to 200 km. The segments are separated by major fault discontinuities, mostly dilational jogs, expressed as valleys and lakes. These segment lengths influenced seismic source dimensions and have limited the magnitudes of large historical fault ruptures to between M_w 6.5 and about 7.7 (Natawidjaja and Triyoso, 2007).

In the past two years, based on current availability of modern digital elevation maps of SRTM-30m and TERRASAR World-30m data, coupled with high-resolution satellite images, Natawidjaja (2017) previously relocated identified active fault strands and identified new fault strands to updated Sieh and Natawidjaja map. New fault strands are particularly added in the northern and southern parts of SFZ where they run toward the Andaman spreading centre and the Sunda Strait grabens respectively (Natawidjaja, 2017; Natawidjaja *et al.*, 2017) (Figure 1). This

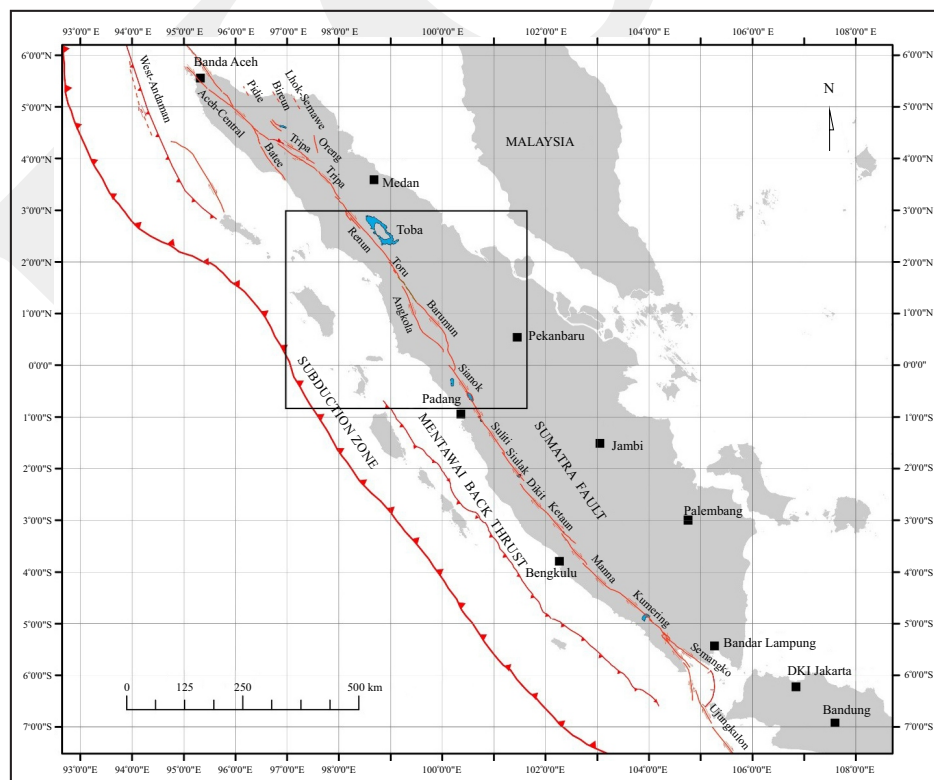


Figure 1. Updated map of the Sumatran Fault Zone (after Natawidjaja, 2017). The bracket marks the central Sumatra region for this study.

study is related to the geological working group activities of the National Team for updating seismic hazard map of Indonesia. The revised seismic hazard maps of 2017 are recently published online at website: <http://puskim.pu.go.id/6901-2/>.

This study presents the latest detailed study on the Sumatran Fault Zone in the central Sumatra region, particularly in Tarutung- Sipirok- Padangsidempuan Area (location marked in Figure 1). The study includes a detailed active fault mapping using high-resolution digital topography with GIS and 3-D imaging technique together with field geological observations of outcrops and landscapes related to active fault movements. Furthermore, it was coupled with geophysical survey using Ground Penetration Radar to image underground structures of suspected active fault zones. The results of this study describe in detailed geometry and kinematics of this fault merging as well as their characteristics and significances to seismic hazards.

SFZ in Central Sumatra

General Structures

The SFZ in central Sumatra is characterized by a major fault bifurcation, where Sianok segment in the equatorial region splits northward into two major strands: Angkola and Barumun-Toru Fault segments, which then they merge into one single major segment, Renun Fault Zone (Figure 2) (Sieh and Natawidjaja, 2000; Natawidjaja, 2003). The Tarutung-Sipirok-Padangsidempuan

area is right on the spot where the fault merging occurs. In general, the Angkola and Toru Faults are not simple, but breaking into smaller fault segments. The previous active fault map by Sieh and Natawidjaja (2000) did not sufficiently depict details of these active fault strands. Hence, this is one of the primary goals of this study.

METHODS AND MATERIALS

Basic Principles of Active-Fault Mapping

A fault is a discontinuity or fracture on the earth crust that shows relative movements of the two separated blocks of rock assemblages. Displacements or slips on active fault movements produce earthquake events. A fault is generally considered active if it shows evidence of movements or seismic activities in Holocene or in the past 11,000 years and in historical-instrumentally recorded period (McClymont, 2001; Kerr and Nathan, 2003; Becker and Saunders, 2005). It can be mapped and studied as it is often illuminated by the earth topographic/landscape or bathymetric expressions, generally as structural lineaments, fault scarps, stream offsets, morphological or geological offsets, and others morphotectonic evidences as well as may serve as a (tectonic) boundary between two different rock formations (Yeats *et al.*, 1997).

The active fault strands can be recognized in the field as they show the following evidences (Yeats *et al.*, 1997):

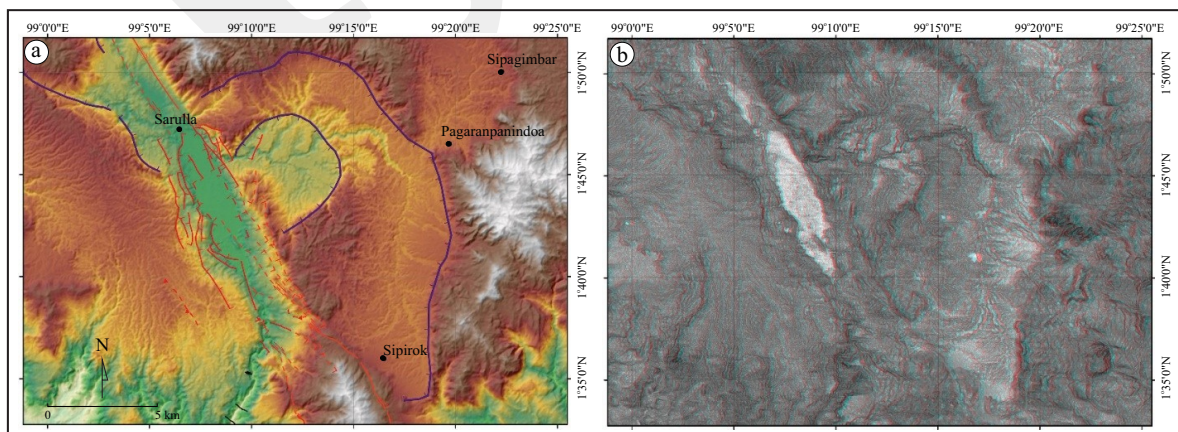


Figure 2. a. Example of SRTM-30m grid DEM data used in this study. b. Example of display for 3-D visualization using “blue and red” eye glasses, located in the Renun Fault Zone.

1. Active fault strands that cut young geological deposits, such as Quaternary volcanic deposits or young alluvium.
2. Fine-scale morphological expressions of fresh fault scarps, linear ridges and valleys, associated morpho-tectonic features such as anticlines, synclines, pressure ridges, hanging valleys.
3. Indication of Quaternary-Recent movements from offsets or deflections of geological or morphological elements such as streams and terraces or human-made features, like fences, roads, *etc.*

Determination of activity of faults in old-pre-Quaternary rock environment is not easy since it cannot be observed whether they cut or deformed Quaternary and Holocene-Recent deposits. An active fault identification based on morphology is also limited by a competition between a rate of movements of a fault and a rate of erosions and depositions. If a fault slip-rate or a rate of movements is very low, lower than rates of deposition and/or erosion, then one may not be able to see as surface-landscape expressions of faults since they will be erased by erosion or buried under geological deposits. The fault zones may still be seen, even when the slip rates are low, if they bound two different rocks with a contrast hardness. Thus, differential erosion rates will highlight the fault. An accuracy of an active fault mapping is also limited by a scale of the base map used. The higher the resolution (*i.e.* the larger the scale) of the base map, the more accurate the mapping, because smaller morpho-tectonic features will be able to be inspected.

Major Tasks

This study has conducted three major tasks, which are:

1. Remote sensing analysis using high resolution topographic data and available satellite images,
2. Geological field survey,
3. Shallow-subsurface geophysical imaging using Ground Penetration Radar survey

to ensure the locations of suspected active fault traces and image their underground structures.

Remote-sensing Analysis for Active Fault Studies

High-resolution digital topographic data base of Sumatra is utilized, including:

- SRTM 30m grids with 3-D visualization software,
- High resolution satellite images from the Google maps,
- Very-high resolution digital topographic LIDAR map (1-m grid) for limited areas along Toru River.

An analysis was conducted using GIS (Geographical Information System) for identifications of active faults, including the use different colour spectrums for changes in elevations, hill shades, and perform contouring analysis for inspecting more detailed relief. In addition, 3-D visualization technique was also used (Katayanagi, 2014) to further identify and map suspected fault strands (Figure 3). The previous active fault map developed by Sieh and Natawidjaja (2000) was revised and modified.

A very high resolution LIDAR (Light Detection and Ranging) digital topography was used for Batang Toru River areas. LIDAR, also called laser scanner, can be conducted with terrestrial or airborne methods. It is a surveying method that measures distance to a target by illuminating the target with pulsed laser light and measuring the reflected pulses with a sensor. Differences in laser return times and wavelengths can then be used to make digital 3-D representation of the target. In particular, at Aek Paya stream, a branch of Batang Toru River, a fresh fault scarp is clearly identified on LIDAR crossing the young alluvial deposits. This has been checked in the field and is confirmed not to be an alluvial terrace, but a linear fault scarp with up to 2 m high rising the north-east block up (Figure 3). Southward from the NW-SE trending fault scarp, the fault line runs across the Aek Paya stream causing a series of small water falls.

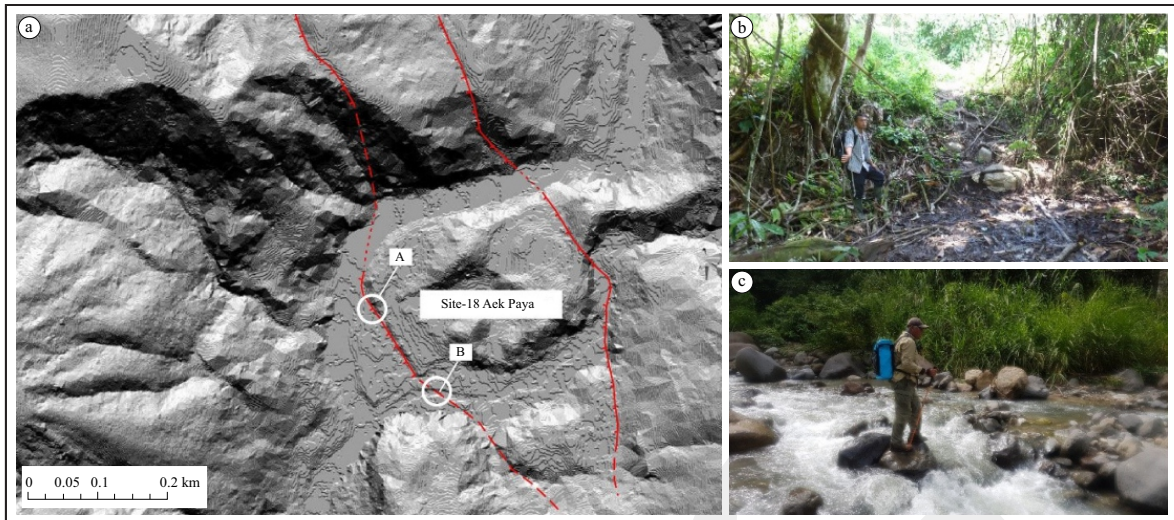


Figure 3. a. LIDAR used to identify small-scale morphological features – fault scarps, an example at Aek Paya, b. Photo of fault scarps at Site 18 Aek Paya, c. Small water-fall steps when fault line across the stream.

Geological Field Survey

The field survey was conducted within fourteen days from 13 to 26 January 2017. It focuses on identifying and characterizing suspected active fault strands in the area between Tarutung-Sipirok-Padangsidempuan where the Angkola and Tarutung Fault zones merged into one.

Ground Penetration Radar (GPR) Survey

To confirm suspected active fault strands and to further investigate their underground fault structures as well as their relations to geological strata, Ground Penetration Radar (GPR) was conducted in selected locations of fault lines that have been identified from remote-sensing inspections and geological fieldworks.

GPR is a geophysical method that uses radar (electromagnetic-wave) pulses to image the subsurface structures. GPR uses microwave band (UHF/VHF) of the high frequency radio spectrum in the range 10 MHz to 2 GHz to detect the reflected and/or refracted signals from subsurface structures/objects/features based on the differences in *permittivities* (similar to electrical/resistivity properties). The depth of the objects/refractors (usually a boundary contrast between two layers/materials) can be estimated from time travels of related waves. GPR can also map plan-view, profiles, or 3D images of features, layers,

and structures. In principle, one-point shoot creates one single electromagnetic waveform that identifies the underground layers characterized by their response of reflecting the waves (Figure 4). Then, many single waveforms along the survey lines are stacked together to create a radargram image. This principle is very similar to the seismic reflection method that is widely used in oil and gas explorations.

A GPR equipment has a main unit that is connected to an antenna, which has a couple set of a source and a receiver. SIR-3000 system from GSSI USA was used and equipped with several kinds of antennas using variety of frequency. Higher frequency provides higher spatial resolution but in the cost of less depth of penetration. Vice versa, deeper penetration can only be achieved by lowering frequency that affects lower resolution. Hence, as most geophysical methods, there is always a trade between resolution and maximum penetration depth. Thus, one always has to set the equipment properly according to targets/goals and site conditions. For this study, the MLF antenna (Figure 4) was used and can be set on the frequency of 15, 40, and 80 MHz to get radargram profiles of moderate to deep subsurface structures from several meters up to 50 m. However, the 40 MHz MLF was mostly used since it gives the best results for this purpose.

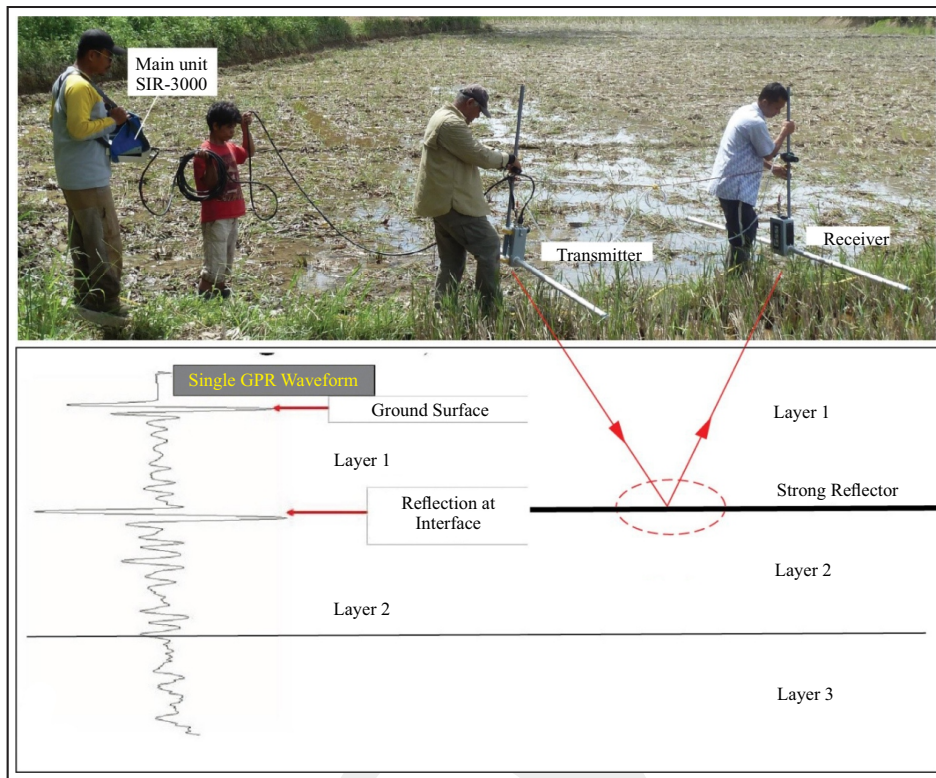


Figure 4. Principles of GPR Suvey using SIR-3000 main unit with MLF Antenna.

If the survey line is not in the flat area, then measuring topographic profile is crucial for topographic correction. Here, the Zip level equipment was used to measure relative elevations using the water-pass principle (Figure 5). Zip level has the accuracy of submillimeter that is comparable to geodetic total station. The advantage of Zip Level is that it is very easy to carry in the field, simple, and it measures fast.



Figure 5. Zip Level for measuring topographic profile along the survey line.

RESULTS AND ANALYSIS

Active Fault Mapping

The surface geology in the studied area is dominated by volcanic products, including the Old-Quaternary and the young Late Quaternary volcanics. The most widespread one is the product of the latest paroxysmal eruption of Toba around 74 Ka, called the Young Toba Tuff (YTT). The tuff occupies most of the north side of Sipirok (Aspden *et al.*, 1982), whilst the southeast side is occupied by the Quaternary Sibual-buali and Lubuk Rata volcanic products. Underlying these Quaternary volcanic products there are dominant Tertiary sedimentary rocks and igneous rocks.

In Padangsidempuan area, the Toru Fault Zone is running parallel to the Angkola Fault Zone, separated about 8 km by the mountainous range that also aligned NW-SE with the SFZ trend (Figure 6). West of the mountainous range, the Angkola Fault Zone is clearly marked by some linear alignments of elongated ridges and longitudinal depressions trending NW-SE across the

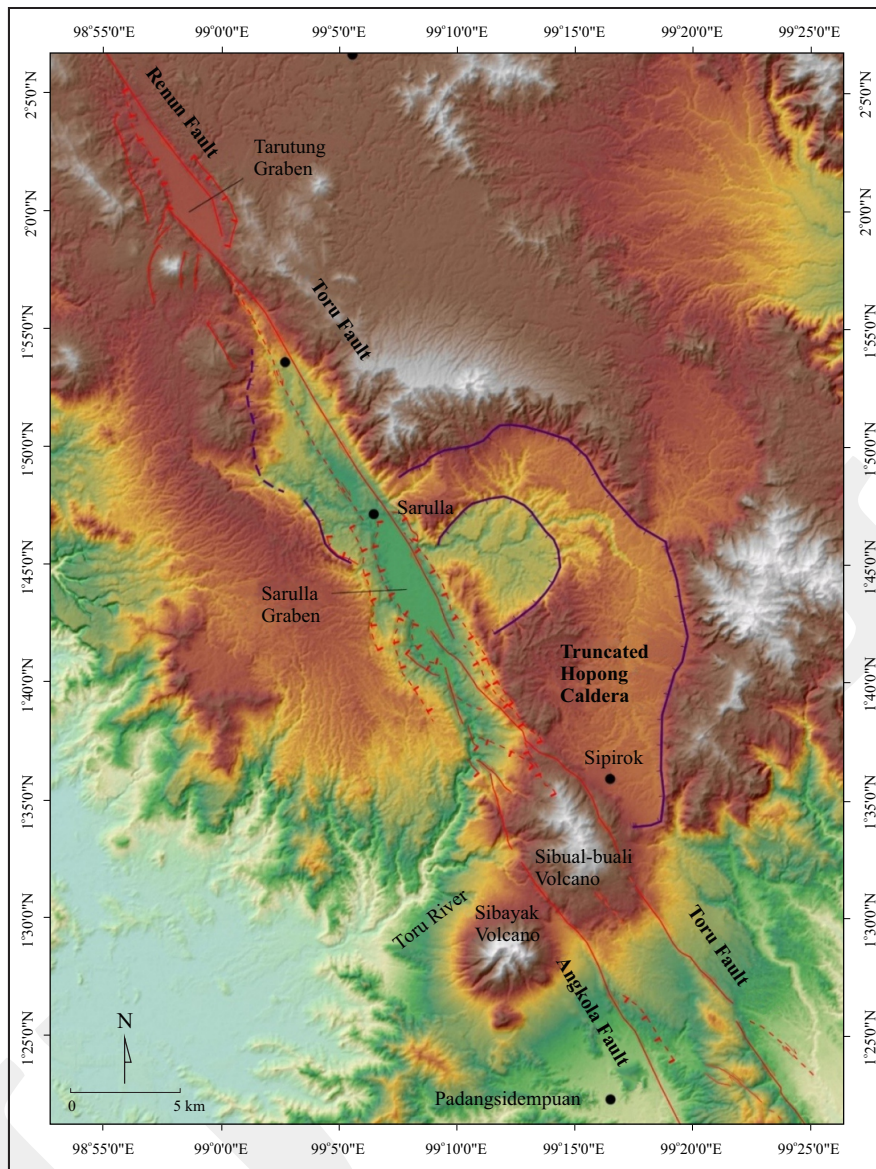


Figure 6. Results of active fault mapping of SFZ between Padangsidempuan and Tarutung areas.

broad valley. The rock exposures at the quarry on the north side of bypass road reveal the Angkola Fault Zone cutting the Quaternary volcanic rock layers and juxtaposed against the sedimentary rock beds (Figure 7).

Along the east side of this mountainous range, from Sipirok southwards to Sibolangit Airport, the Toru Fault Zone generally runs as a single major strand, characterized by linear ridges, linear scarps, and linear valleys. In a few locations, the fault strands are also marked by the appearances of small lakes or ponds indicating segmentations or pull-apart stepover along the fault. The largest

depression is Tasik Lake, located about 5 km west from the Sibolangit Airport. The Lake is about 600 m long and 400 m wide (Figure 8). The shape of the lake clearly indicates that it is formed as a *pull-apart basin* (Figure 13).

The Angkola Fault runs northward cutting the southwestern side of Sibualbuali Volcano, and then it is broken into smaller segments forming a series of normal faults enveloping the NW-SE elongated Sarulla Graben (Figure 6). From Sarulla northward approaching Tarutung, the Angkola Fault gradually merges onto the Toru Fault before it bounds the southern edge

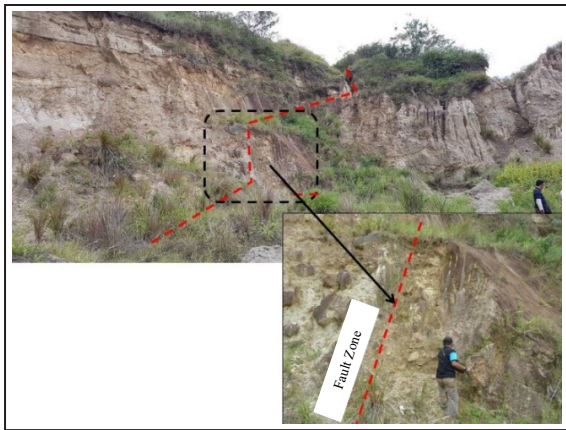


Figure 7. The Angkola Fault Zone is exposed on the rock quarry at the coordinate of 1.804324 S, 99.10611E at the north side of the bypass road.



Figure 8. Lake Tasik pull-apart depression. Photo faces northwestward, situated 5 km westwards from Sibolangit Airport.

of the pull-apart Tarutung Graben as the northern termination of the Toru fault with the Renun fault segments in the north side.

A very large Early Quaternary Caldera with a diameter of about 9 km, called the Hopong caldera (Hickman *et al.*, 2004), is spectacularly truncated along the SFZ or the eastern edge of Sarulla Graben between Sipirok and Sarulla (Figure 6). The Hopong Caldera, based on $^{40}\text{Ar}/^{39}\text{Ar}$ dating of a plagioclase mineral separated from welded rhyodacite ash-flow tuff, was formed during a major volcanic eruption about 1.46 ± 0.12 Ma (Hickman *et al.*, 2004). Large parts of this ancient caldera and its products have been covered by the 0.73 Ma Young Toba Tuff (YTT) layer.

Outcrops of the Toru Fault Zones are exposed in several places along the main road between

Tarutung and Sipirok. Exposures on the new-road cliff reveal a series of normal faulting associated with Toru Fault Zone indicating a significant fraction of extensional deformation (Figure 9). Near the intersection between the new and old roads, a few kilometers north of Sipirok, the main Toru strike-slip Fault Zone is clearly exposed on the road-cut cliff and it obviously cut and deformed the road asphalt (Figures and 10 a, b, c). This road is repaired repeatedly. Another excellent exposure is on the road from Sipirok southwestwards along the Toru River, where the asphalt road is also cut and deformed by the Toru Fault Zone (Figure 10 d). These evidences strongly indicate that the Toru Fault is creeping, or continuously moving (aseismically).



Figure 9. Exposure of extensional faulting associated with Toru Fault Zone along the new-road cliff near Sipirok (Site 8 - location marked at Figure 13).

Geothermal Features

There are many geothermal activities in the region of the dam site, including hot springs and fumaroles (Gunderson, 1995, 2000; Hickman *et al.*, 2004). Based on field investigations and mapping, locations of geothermal occurrences are mostly, if not all, related to the fault zones. Hence, they can be used as markers for identifying active fault strands.

A large part of geothermal fields appears to have occurred along the boundary between Renun and Toru Fault segments. The largest and most beautiful site is the Simolohon hot spring in the town of Tarutung, which is located at the southern end of Renun Fault, where it bounds the east-side edge of the Toru depression, an extensional stepover between Renun and Toru



Figure 10. Exposures showing deformed asphalt roads due to creeping fault zones. a, b, and c are at Site 9 - new road route near Sipirok; d. is at Site 5 - on the road from Ikan Bakar Restaurant in Sipirok going southwest along Toru River. Location of Site 9 and Site 5 are marked in Figure 15.

Fault segments (Figure 11a). Near Sipirok, the geothermal field is also observed next to the main road at Site-2 (location marked in Figure 12). Here, geothermal fluids come to the surface through the Toru main fault, burning the soils and trees that becomes black coloured. A large geothermal field, especially hot springs, occur at Aek Nabara (in local language it means a burning river) (Figure 11b). It is located at the southern end of the Angkola Fault.

GPR Survey

To locate exact locations of fault lines and to explore their underground structures in relation with stratigraphy, GPR surveys have been conducted in selected sites, where the locations of the fault lines have been estimated from a tectonic-landscape analysis (Figure 14). Below are the results of GPR surveys together with their geological field observations.

Site 3

Site-3 is located at the major Toru Fault, about 2 km north of the Sarulla Town near the northern edge of the truncated Hopong Caldera (north of Site 4 in Figure 12). Here, the fault zone is characterized by a linear valley about 200 - 250 m wide, now occupied by rice fields (Figure 14a). GPR was conducted across the valley to investigate the precise location of the fault zone. The results reveal two major strands of the fault in both sides of the valley (Figure 15a). This indicates that this longitudinal valley formed as a graben structure between two faults with significant normal movements. The faults cutting through young Holocene sediments confirm that this is a very active fault zone.

Site 7

Site 7 is situated in Purbatua Village. This ground-check point is to investigate the fault that is a continuation of the Aek Paya Fault, shown in

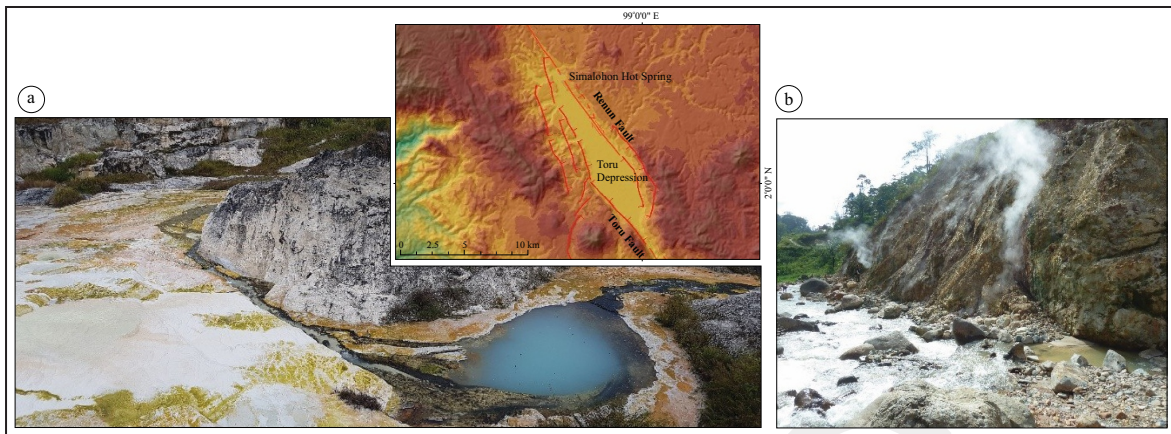


Figure 11. Examples of geothermal exposures associated with the fault zone; a. Simalohon hot spring in the town of Tarutung associated with Toru Fault; b. Aek Nabara hot spring associated with Angkola Fault (location marked in Figure 12).

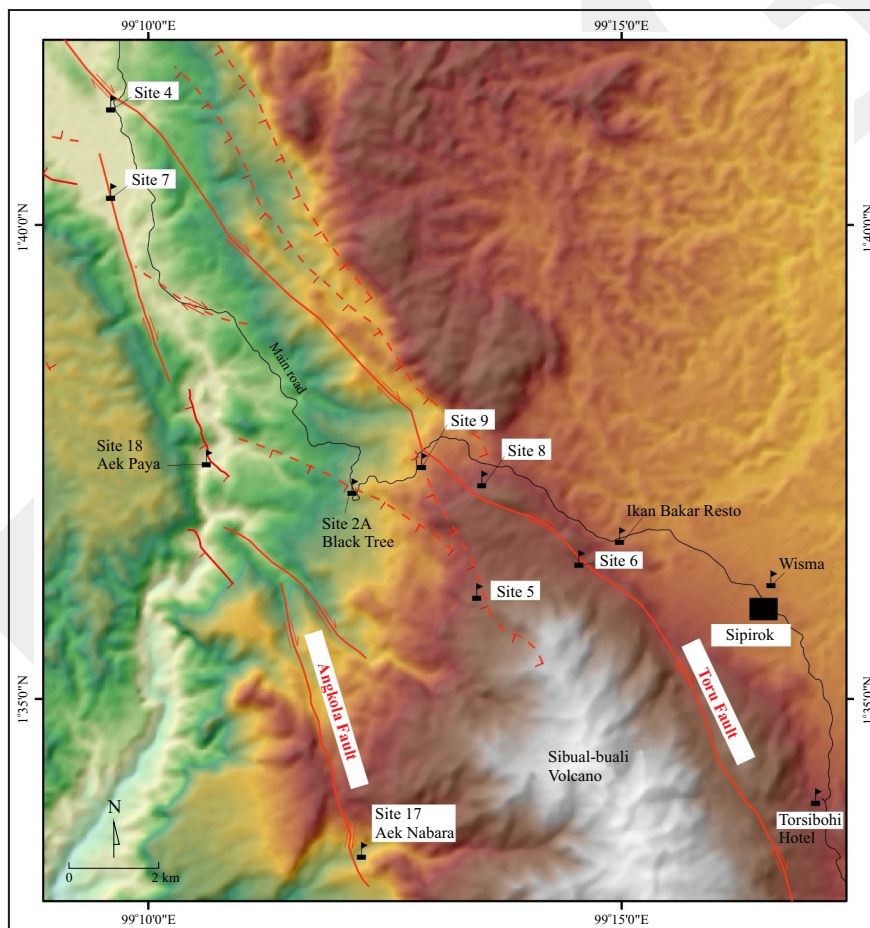


Figure 12. Active fault and site index map for Sipirok-Sarulla region.

Figure 12. Morphologically, the site is a depression, now occupied with rice field, in between the two linear ridges (Figure 14b). Hence, the fault line is expected to lie somewhere in the rice field. The GPR survey across this rice field

is about perpendicular to the fault line. The radargram or the result of the GPR survey shows clearly the existence of the active fault that cut the young alluvial deposits beneath the rice field (Figure 15b).

Major Bifurcations, Slip Rates, and A Creeping Segment of Sumatran Fault Zone in Tarutung-Sarulla-Sipirok-Padangsidempuan, Central Sumatra, Indonesia (D.H. Natawidjaja)

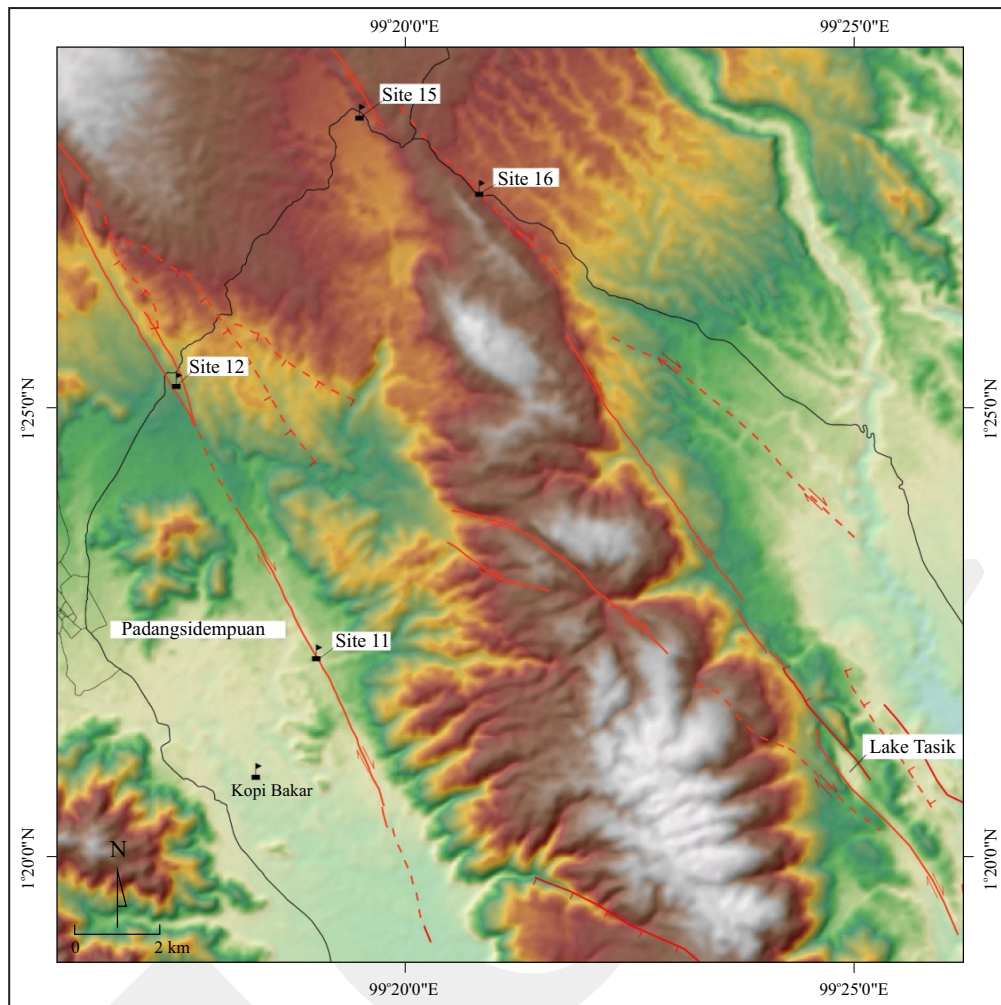


Figure 13. Active fault and site-Index map of Padangsidempuan region.



Figure 14. Photos of GPR surveys at selected locations. Black dash-lines are estimated locations of fault line based on a morphology analysis. a. Site 3; b. Site 7; c. Site 8; d. Site 6; e. Site 10-11 .

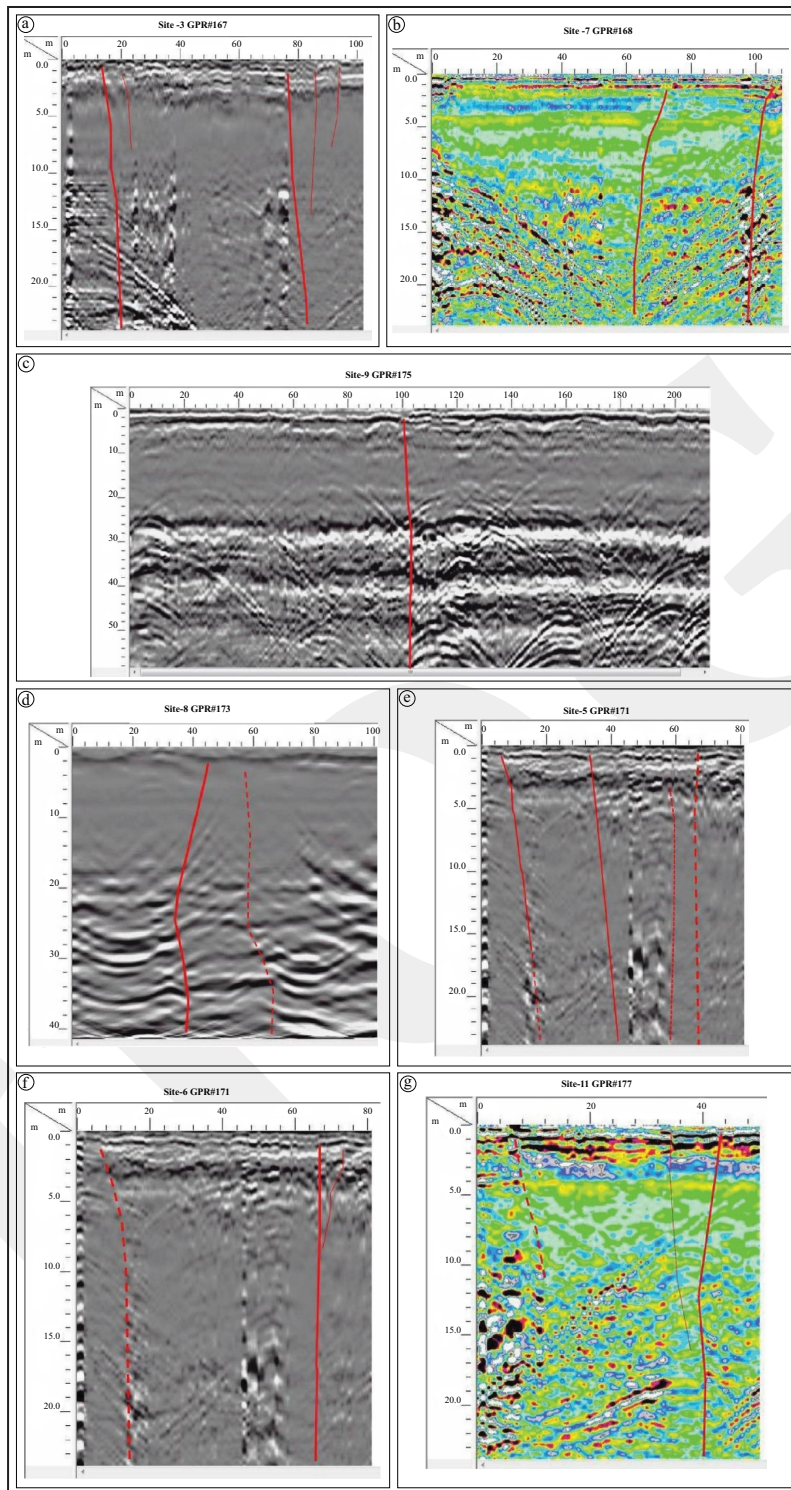


Figure 15. GPR Profiles (radargram) from: a. Site 7; b. Site 9; c. Site 8; d. Site 5; e. Site 6; f. Site 3; g. Site 10-11.

Site 9

Site-9 is on the new road, south of Sipirok, which is continuously deformed due to slow ground movements (Figure 12). Our mapping shows that this site is located on the main fault

strand of the Toru Fault Zone. The fault zone is exposed on the road cliff right near the deformed asphalt road. The fault clearly juxtaposed the rock breccia layer and the tuffaceous sand layer (Figures 10 a, b, c). Thus, the Toru Fault is ac-

tive moving slowly in an aseismic mode (*i.e.* not producing earthquake).

The GPR survey runs by passing through the fault line crossing the road. The underground structures revealed on GPR profile showing that the fault strand cuts through the soil and rock strata beneath the road (Figure 15c). Hence, it confirms the location of the Toru Fault and its recent movements.

Site 8

Site 8 is about 1 km eastward from Site 9. There is a new road construction made a cut through the hill, exposing the rock layers and structures on the road cliffs on both sides along the road cut (Figure 12). The rock strata appear to be folded, forming an anticline, and is cut by a fault zone near the crest line dragging and deforming the layers on both sides. The layers on its east flank are cut by a series of normal faults that steeply dipping toward the main fault (Figure 14c). Hence, it indicates that it is a negative flower structure, which is part of the Toru Fault Zone. The GPR survey runs along the road crossing the anticline and the fault zone. The result illuminates the subsurface structures of the fault zone that cut the layers into the deep (Figure 15d).

Site 5

Site-5 is located at an asphalt road from the Ikan Bakar Restaurant in Sipirok, southwestward along the east side of Batang Toru River (Figure 12). The asphalt road at site-5 is also continuously deformed along the fault (Figure 10d). The GPR survey along the road passed through this fault line, marked by the large crack crossing the road. The result confirms that this surface crack associated with several parallel fault strands that cuts the soil and rock strata underlying the road (Figure 15e). These faults are part of the secondary normal faulting that deviates from the main Toru Fault Zone.

Site 6

Site-6 is situated on the same road, about 2 km towards east from Site-5, and only about 800 m to the west from the entry point at the main road near the Ikan Bakar Restaurant (Figure 12). This

site is at the main Toru Fault Zone, characterized by a linear ridge along the east side of the fault strand. The fault line cuts the road at a low angle (Figure 14d). Indications of fault creeping are not observed at this location (Figure 15d). The GPR survey at this site reveals two fault strands beneath the road (Figure 18f).

Site-11

From Toru River, the Angkola Fault which runs southwards mostly as a single major fault line bisecting the saddle area between Lubukrata and Sibualbuali Volcanoes (Figure 13). Site-11 is selected at this major fault line about 5 km east from the city centre of Padangsidempuan. The fault zone can clearly be identified from linear ridges and fault escarpments, and longitudinal valleys. In some spots, it is also marked by ponds that are associated with fault segmentations. Sites-10 and 11 are located at a straight narrow depression between a linear ridge and the linear escarpments of the highland along the east side, which is now occupied by rice fields (Figure 14e).

A GPR survey was conducted to scan the precise location and detailed subsurface structures of the fault beneath the valley or rice field. The result of GPR profiling displays two main fault strands at both east and west-end sides of the survey line, indicating that the linear valley are bound at both sides by faults (Figure 15g). Thus, it is a graben-like structure. The fault zone cuts/deforms the young alluvial deposits that are akin to its recent fault movements/activities.

Fault Slip Rates

Kinematics and level of activity of active faults are primarily measured by their slip rates or how fast they move. For this purpose, slip rates were evaluated on three principle locations, which were on: 1. Renun Fault at the northern side of the fault bifurcation, 2. Sianok Fault at the southern side of the fault bifurcation, 3. The Fault bifurcations: Toru and Angkola fault segments.

Slip Rates on Renun Fault, Toba Lake

The Renun fault traverses from 3.55°N southwards to 2.0°N along the western flank

of the 80-km-long Toba Caldera (Figure 16), alleged to be the largest Quaternary caldera on earth (Chesner *et al.*, 1991). Much of the fault traces deeply entrenched the thick pyroclastic flow deposit of the 74,000-year-old Toba eruption (Figure 17). Renun Fault length is measured about 220 km long, the longest segment of the SFZ. Therefore, it is considered to be capable of generating earthquakes up to magnitude Mw 7.8 if the entire fault length is ruptured during a single major earthquake.

It is clear that the Young Toba Tuff (YTT) flow sheet reset the previous landscape by effectively buried the pre-existing topography upon emplacement. Then, this instantaneous burial of

tens of square km of territory followed by the fast creation of a new network of drainages across the trace of the SFZ. Thus, the wide-spread YTT where the faults cut through the new drainage system gives unique opportunity for conducting slip rate measurements by finding good fault offset of drainage channels, and then divided by the age of YTT that was emplaced from the latest super volcano eruption.

The age of YTT eruption has been very well defined by multiple analyses from previous studies. Ninkovich *et al.* (1978) dated sanidine and biotite in welded tuffs using K-Ar dating yields 73.5 ± 3 ka and 74.9 ± 12 ka respectively. Chesner *et al.* (1991) also dated sanidine of YTT by using

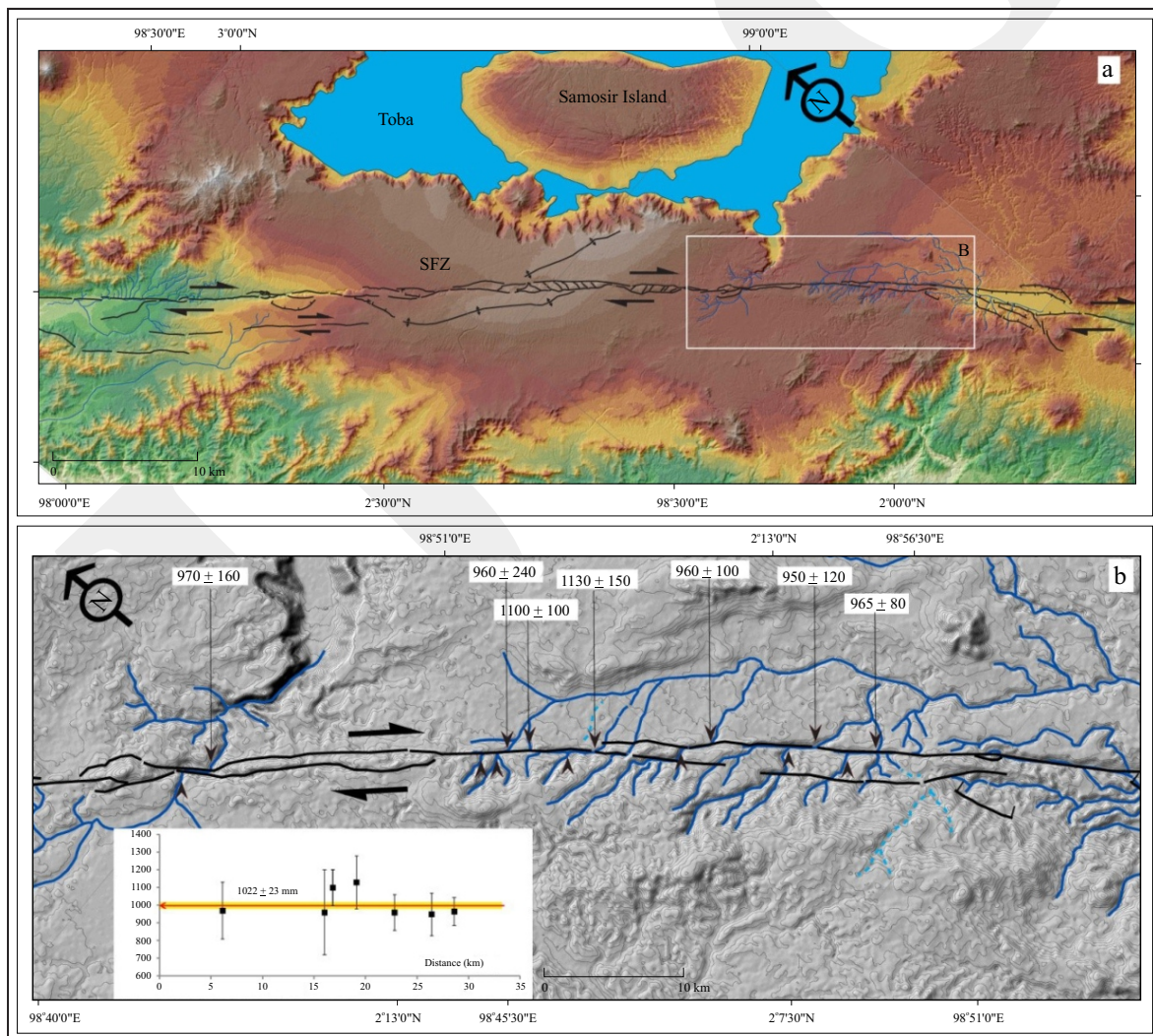


Figure 16. a. The Renun segment of SFZ traverses the thick Young Toba-Tuff (YTT) plain in the SW side of Toba Lake, b. Several river canyon network incising into the 73.8 ± 0.4 ka YTT are isochronously displaced about 950 to 1,100 m with an average of $1,022 \pm 23$ m. It yields a slip rate of 13.8 ± 0.3 mm/yr. Colour and shaded relief map is from SRTM 30.

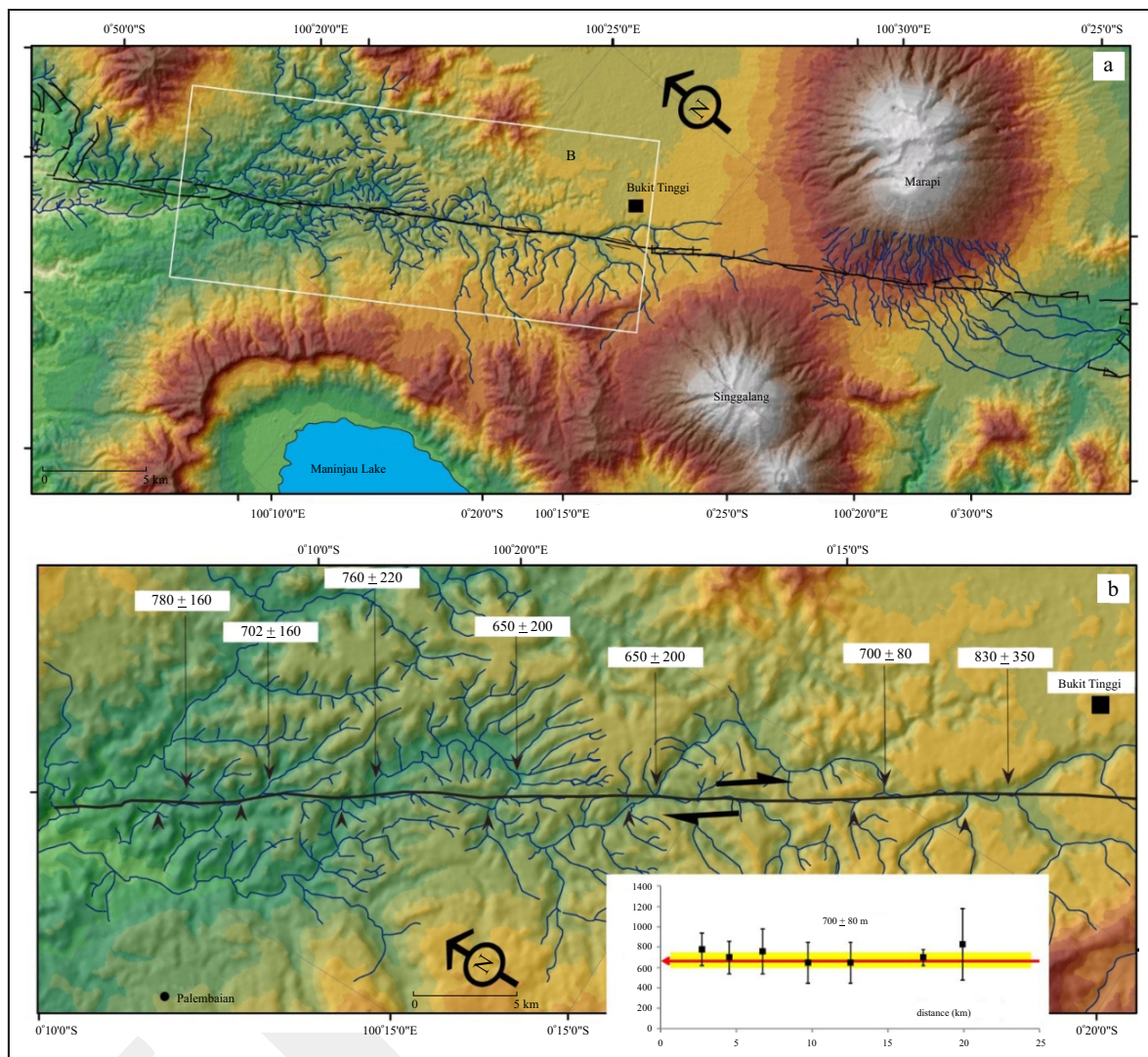


Figure 17. Sianok segment of SFZ traverses the thick Maninjau Tuff (YTT) on a plain between Maninjau Lake and Marapi Volcano, B. Showing that seven deep river channels that had incised the tuff and isochronously offset about 700 m in average by the fault movement. It yields a slip rate of 13.7 ± 1.6 mm/yr.

$^{40}\text{Ar}/^{39}\text{Ar}$ method and they yielded 73 ± 8 ka. Mark *et al.* (2014) also using $^{40}\text{Ar}/^{39}\text{Ar}$ method on sanidines separated from pumices of the proximal YTT obtained an eruption age of 74.2 ± 1.8 ka. They also used the same method, but on a very fine-grained biotite separated from ash beds exposed on Peninsular Malaysia, and they obtain eruption ages of 73.9 ± 8.8 ka and 72.7 ± 8.2 ka. Storey *et al.* (2012) also used $^{40}\text{Ar}/^{39}\text{Ar}$ method on sanidine grains separated from a Malaysian ash bed, obtaining a 73.88 ± 0.64 ka, although Mark *et al.* (2013) suggested revision of this age to 74.2 ± 0.8 ka using a different astronomical calibration of the $^{40}\text{Ar}/^{39}\text{Ar}$ geochronometer.

Hence, a nonweighted average of those ages is 73.8 ± 0.4 ka (2σ) (Bradley *et al.*, 2017).

The southeastern part of the Renun Fault segment exhibits excellent isochronous river offsets along the major fault strand. Sieh *et al.* (1994) measured about 2-km offsets of several river channels that deeply incised the $\sim 74,000$ -year-old Young Toba Tuff (YTT), which they have used to determine a 27 mm/yr geological slip rate for the fault.

The previous GPS-campaign measurements that across the southern portion of this segment suggest geodetic slip rates of 24 ± 1 mm/yr (at about $N 2.7^\circ$). Another one that across the

northern portion of the Renun segment yields a geodetic rates of 26 ± 2 mm/yr. (at about $N 2.2^\circ$) (Genrich *et al.*, 2000). Hence, the geodetic and the geological slip rates seem to be concurred.

However, Bradley *et al.* (2017) re-analyzed the isochronous river-channel offsets along the southern portion of the Renun Fault and concluded that the most likely case is ~1-km pairs of offsets, not the 2-km offsets that were previously suggested. Bradley *et al.* (2017) results show that the average offset of five channels incised into the tuff along the southern and northern parts of this fault segment is 1043 ± 36 m. This yields a post-eruption right-lateral slip rate of 14.1 ± 0.5 mm/yr.

This study results also suggest a very similar average offset of river channels of 1022 ± 23 m (Figure 16). Hence, considering the estimated average age of YTT about 73.8 ± 0.4 Ka as the approximated time of the initial incision of the YTT after the eruption, and taking into account error propagation due to uncorrelated and random uncertainties of the offset measurement (δd) and time of initial incision (δt), the slip rate, v , can be calculated as follow:

$$v = d/t, \text{ and uncertainty in slip rate,} \\ \delta v = v * [(\delta d/d)^2 + (\delta t/t)^2]^{0.5}$$

Where: $d = 1022$ m; $t = 73.8$ ka; $\delta d: \pm 23$ m; $\delta t = \pm 0.4$ ka (ka = thousand years ago).

Hence, slip rate on the Renun segment is 13.8 ± 0.3 mm/yr. Thus, this suggests only about half as much as the slip rate value that was previously suggested by Sieh *et al.* (1994), and is very similar to that of Bradley *et al.* (2017).

Bradley *et al.* (2017) also developed a new kinematic model for Sumatra and recalculated geodetic slip rates along the SFZ. They use the latest available kinematic data from GPS campaign measurements, continuous GPS network SuGAR (Sumatran GPS Array), and also from coral-paleodetic data. Their results estimated slip rates for purely strike-slip segments of the Sumatran Fault vary between 14.8 and 16.9 mm/yr, with locally lower rates that coincide with

large restraining or releasing bends where significant across-fault motion is expected. At latitude around Toba, the crustal-motion geodetic model and the 2D geodetic-elastic model across Toba yields the best-fit geodetic slip rates suggest a slip rate at approximately 14.7 mm/yr. Thus, these re-modelled geodetic slip rates are also in favour with the new geological slip rate measurements.

The key point to this discrepancy is that the previous geodetic studies, which yielded higher slip rate values on Sumatran strike-slip fault (Genrich *et al.*, 2000), appear to have neglected the trench-parallel motion of the fore-arc islands arising from oblique loading of the Sunda megathrust. In other words, since the latest kinematic model that takes into account trench-parallel slip motion on the megathrust, it yields lower slip motion on the Sumatran Fault.

Slip Rates on Sianok Fault, Maninjau Lake

In West Sumatra around Bukittinggi, the Sianok segment of the Sumatran Fault traverses the Maninjau Tuff that was erupted during the formation of Maninjau Caldera and subsequently incised by the Sianok and Palupuh Rivers (Sieh and Natawidjaja, 2000). The Maninjau Tuff has been dated by a combination of ^{14}C and glass fission track (GFT) techniques (Alloway *et al.*, 2004). Bradley *et al.* (2017) estimated an eruption age of 51.1 ± 0.9 ka, calculated as a non-weighted mean of the ^{14}C and GFT ages.

East of the Maninjau Caldera, the sinuous Sianok River crosses the Sumatran Fault at moderate to high angle at seven separate locations (Figure 17). The amount of the offsets ranges between 650 m and 830 m. The uncertainty for each offset measurement was estimated as approximately the width of the offset river channels, which is on the order of 160 to 350 m. Hence, applying statistical calculation, the average value of the offset is 700 ± 80 m. Using the similar mathematical formula above, the slip rate calculated from these seven isochronous river-channel offsets is 13.7 ± 1.6 mm/yr. This is very similar to that which has been calculated by Bradley *et al.* (2017), that is about 14 mm/yr.

Slip Rates at the Bifurcation Structure: Toru And Angkola Faults

Hickman *et al.* (2004), based on a detailed geological mapping, observed that Tor-Sibohi Rhyodacite dome with a diameter of about 3.5 km, a few kilometer southwest of Sipirok, was dextrally offset along the major Toru Fault (or the Tor-Sibohi Fault as they called it) about 2.1 to 2.9 km (or $\sim 2.5 \pm 0.4$ km) (Figure 18). The age of the rhyodacite dome, based on incremental heating $^{40}\text{Ar}/^{39}\text{Ar}$ dating method on biotite mineral, is $0.27 \pm 0.03\text{Ma}$ (Hickman *et al.*, 2004). Using a similar calculation as above, this yielded a slip rate of 9.3 ± 1.8 mm/yr. Since the fault slip rates on the south and the north sides of the bifurcation are similar, which are 13.8 ± 0.3 mm/yr and

13.7 ± 1.6 mm/yr for the Renun and Sianok Fault segments, then the total slip rate across Toru and Angkola segments must also be about $\sim 13 - 14$ mm/yr. Thus, the slip rate on the Angkola Fault is about $\sim 4 - 5$ mm/yr.

Earthquakes

Historical Seismicity

There are several major historical earthquakes occurring in the central Sumatra region. Hurukawa (2014) relocated these earthquakes including those pre-1960 events from old analog seismogram data. The relocated epicentres and magnitudes of these earthquakes are shown in Figure 19. The largest historical earthquake event ruptured the Angkola Fault with estimated magnitude of up to M7.7 in

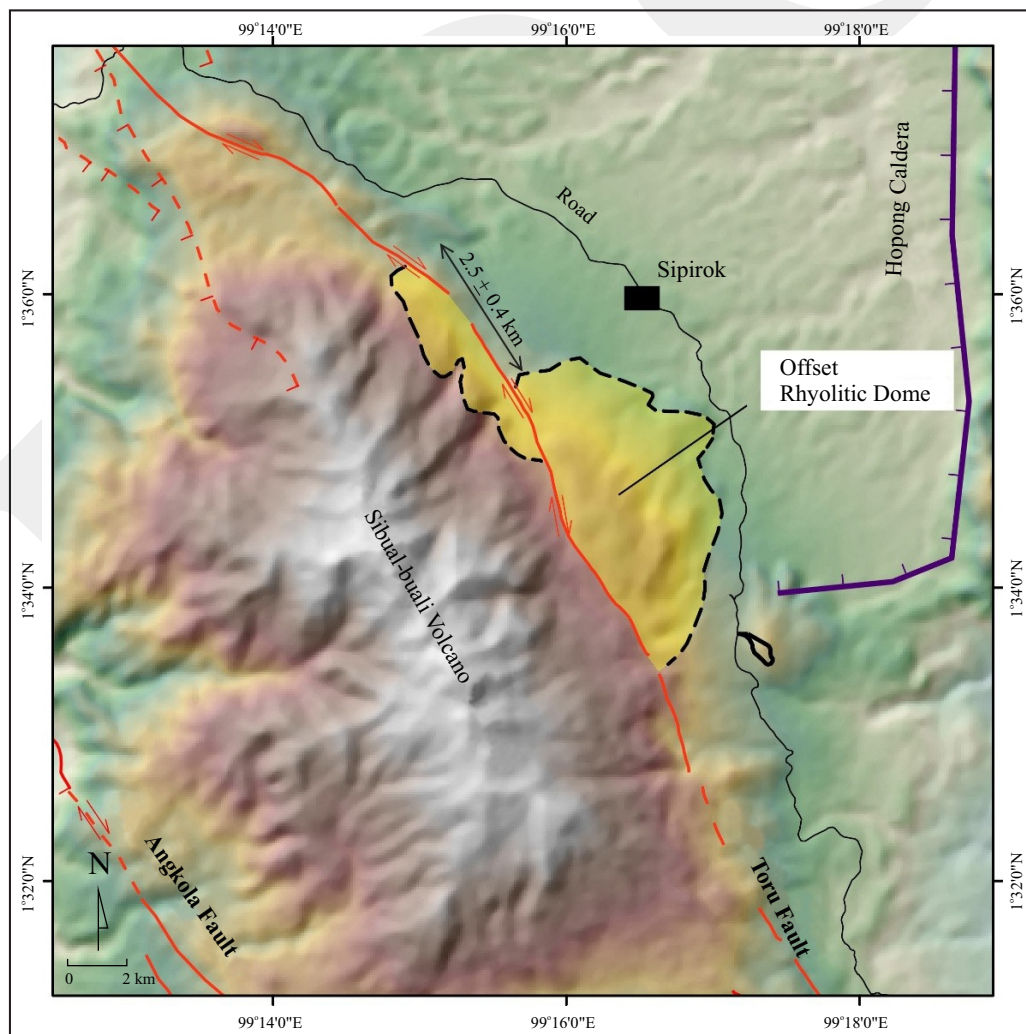


Figure 18. The 0.27 Ma (=270 ka) rhyolitic dome is dextrally offset about ~ 2.5 km along the Tor-Sibohi Fault or Toru Fault segment. Map of the offset rhyolitic dome is re-drawn from Hickman *et al.* (2004) and plotted on SRTM 30 in this study.

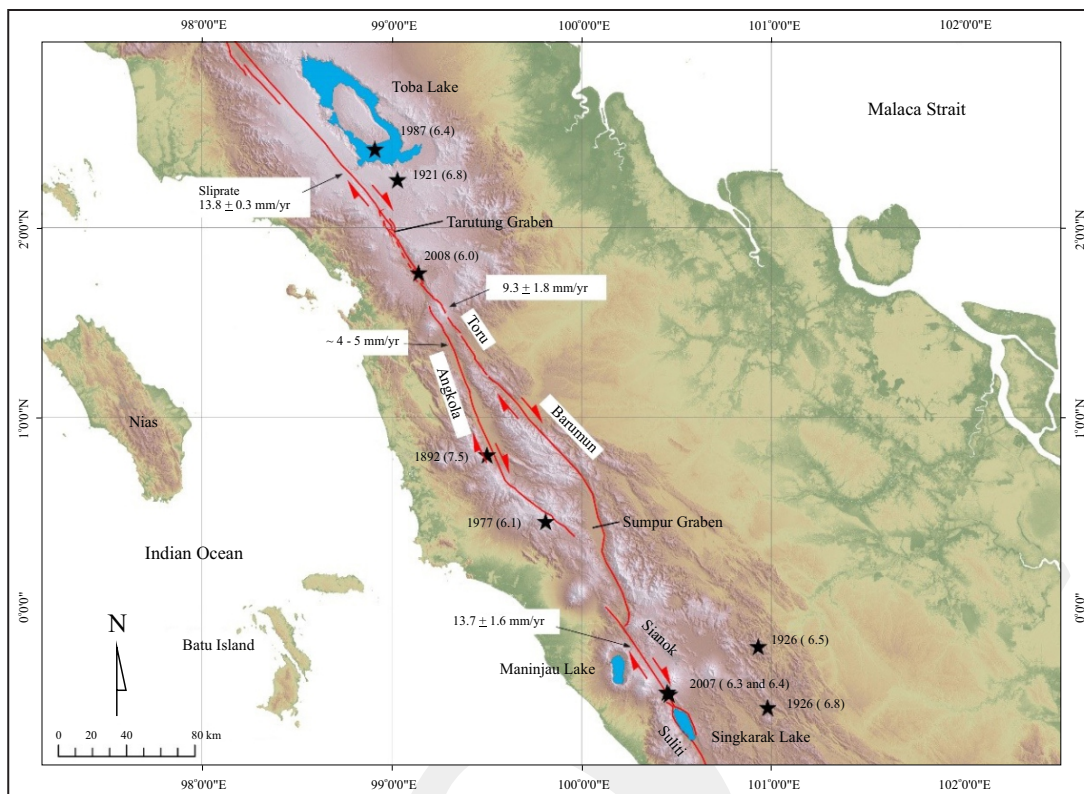


Figure 19. SFZ in Central Sumatra region with slip rates from this study. The black stars are relocated epicentres of past earthquakes along the Sumatran Fault Zone (Hurukawa, 2014).

AD 1892 based on the damaged area or earthquake intensity, and data of fault slip displacement was recorded by surveying the old geodetic triangulation networks (Prawirodirdjo *et al.*, 1999). Other major earthquakes occurred along the Renun segment in 1916 and 1921 (~M7). Note that the Toru Fault has not produced earthquake with magnitude of larger than M6.5. The largest earthquake here occurred in 1984 (M6.4) around the town of Tarutung. More recent earthquake occurred around *Sarulla Basin* in 2008 (M6). In the south, the 1926 (M6.5 and M 6.8) - twin earthquake event ruptured Suliki and Sumani segments around Singkarak Lake. In 2007, the twin events occurred again on the similar segments like the 1926 event (Daryono *et al.*, 2012).

Instrumental Seismicity

Seismic activities on the Renun, Toru, Angkola, Barumun, and Suliti-Sianok Fault segments are shown by plots of earthquake epicentres from EHDL catalog from 1964 to 2009 (Engdahl,

2007) (Figure 20a). For the highlight, a cluster of small earthquakes occurred on Toru segment. Weller *et al.* (2012) had recorded micro-seismicity with the magnitude from M1 to M3.5 between 2008 and 2009 from their temporary seismic networks along SFZ from Toba Lake to South Sumatra (Figure 20b). On this higher accuracy of seismic observation, a cluster of earthquake or earthquake swarms occurred along a narrow zone right on Toru Fault indicating that this fault segment is probably creeping. Another important aspect, there is a widely distributed micro-seismicity on a highland sandwiched between Angkola and Barumun Fault Zones. This may imply that the block is broadly deforming due to movements of the two major faults. Another cluster of swarm earthquake occurred in the area between the Sianok and Suliti segments in the vicinity of Singkarak Lake. This earthquake swarm is post seismic activities after the 2007 earthquake doublet that ruptured both Suliti and Sianok segments (Daryono *et al.*, 2012).

Major Bifurcations, Slip Rates, and A Creeping Segment of Sumatran Fault Zone in Tarutung-Sarulla-Sipirok-Padangsidempuan, Central Sumatra, Indonesia (D.H. Natawidjaja)

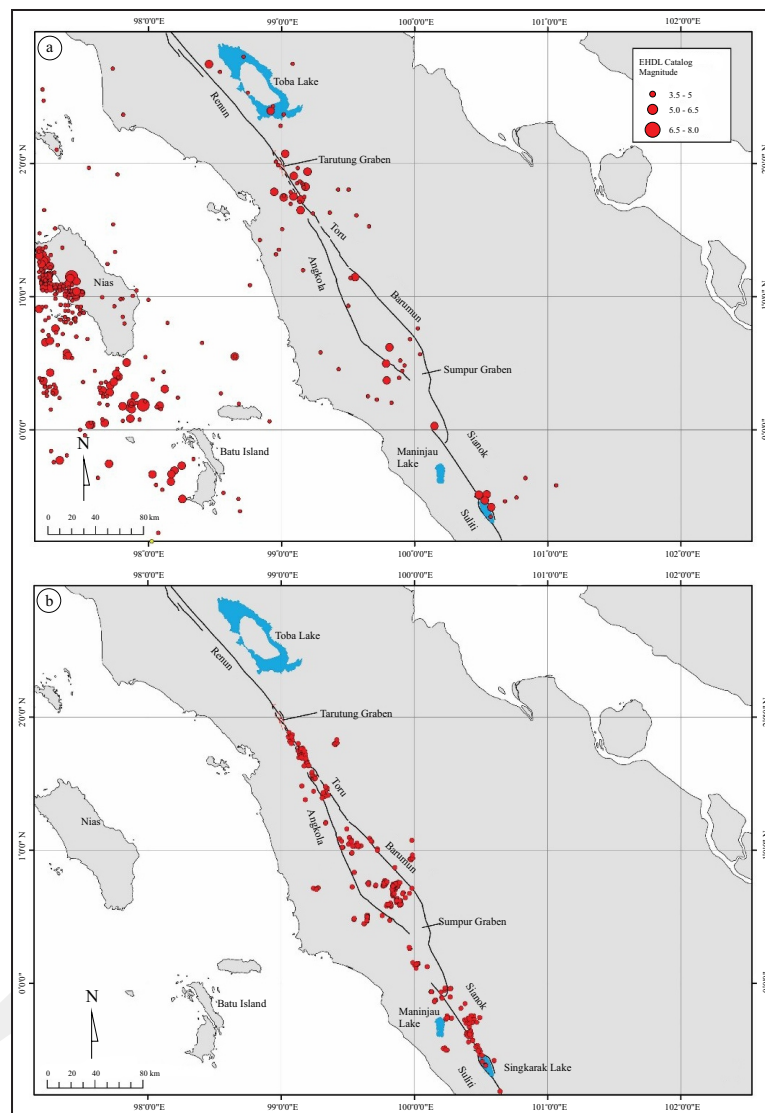


Figure 20. Plots of earthquake events with depth up to 30 km from: a. EHDL catalog (1964 - 2009) and b. recorded by a temporary seismic network, deployed from 2008 to 2009 from Weller *et al.* (2012).

DISCUSSION

One crucial observations, Toru Fault around Sarulla - Sipirok area is strongly indicated to have been creeping. This may be supported by the fact that in the historical record, the ~100-km-long Toru Fault segment did not produce some comparable large earthquakes (Magnitude 7 or larger) but only M6 earthquakes. In contrast, the adjacent SFZ segments, Renun and Angkola segments, did produced large earthquakes. Fault creeping segments has been known worldwide. The most famous fault creeping segment is the Park field

section of the San Andreas Fault in California (Ben-Zion and Malin, 1993). Park field fault section had also produced earthquakes with magnitudes only M6 since 1800s with an average regular interval of every 22 years, while the adjacent segments had produced M8 earthquakes with much greater recurrent interval (Bakun and Lindh, 1985; Bakun and McEvilly, 1984). This creeping aspect is critical for understanding the kinematics and tectonics as well as its significant to fault and seismic hazards.

Speaking of seismic hazards, the Sarulla geothermal power plant facilities are built right on the zone, sandwiched by the two major Toru and Angkola Fault Zones (Figure 21). Thus, this

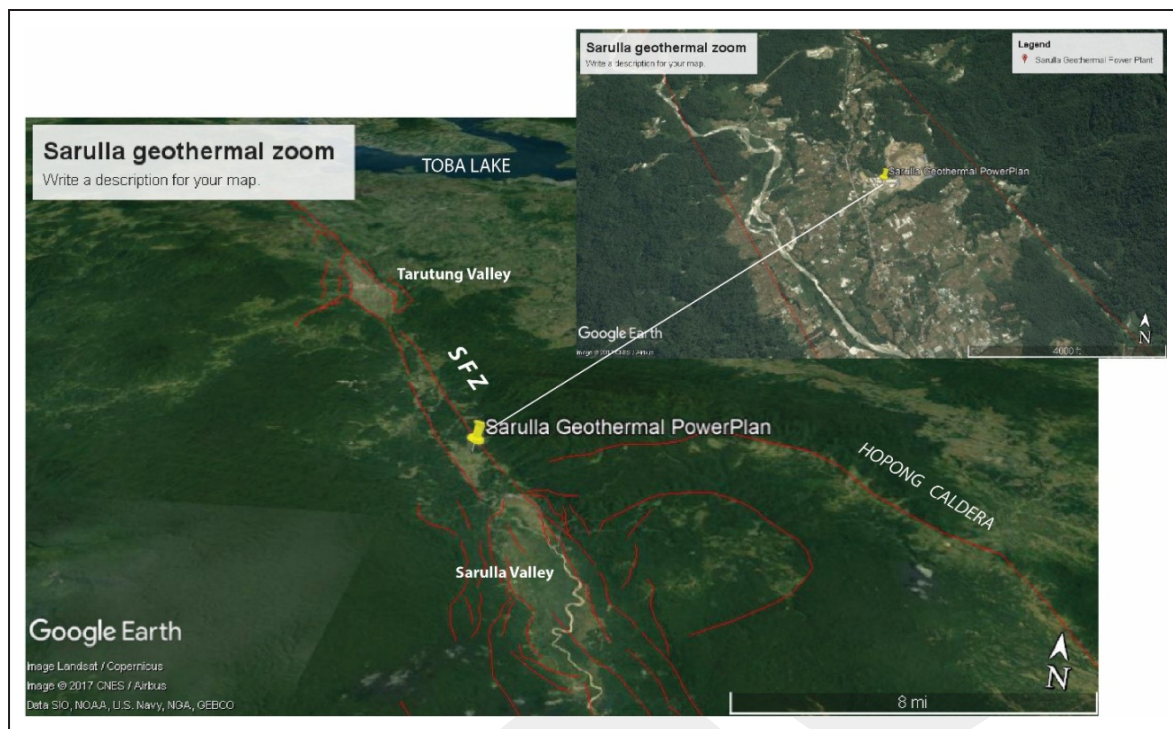


Figure 21. Plots of active faults and the location of the Sarulla Geothermal power plan on the Google-Map satellite images.

power plant has a very high seismic risks, not just from severe shaking during a major earthquake event but possibly also from ground deformations due to fault surface ruptures. Hence, future much details study on the locations and characteristics of the Angkola and Toru Fault Zones is crucial for the safety of this mega installation and people live in this area.

CONCLUSION AND RECCOMENDATION

This study has demonstrated the method to study active faults. It shows that active fault strands in the region are recognizable on SRTM 30 from their morphological features. Advanced technique, such as using 3D imaging of SRTM 30 also helps to visualize morpho-tectonic features. Very high resolution DEM, such as LIDAR is indeed very useful for identifying and mapping small-scale active tectonic features, such as up-to-2m fault scarp at Aek Paya. The GPR survey that has been used in this study is proven to be effective in identifying and localizing accurate location of active fault lines/zones.

The results of this study has mapped in great details the active faults in the region of Tarutung - Sarulla - Sipirok - Padangsidempuan where the SFZ two major strands: Barumon-Toru and Angkola segments are runs (sub) parallel and then merging slowly into one zone at Tarutung pull-apart depression, and then becomes one major Renun Fault Zone in Toba-lake area. There are few major features observed:

- The block area between Angkola and Tarutung is somewhat complexly deformed, dominated by extensional deformations in the study area. These includes the formations of large Sarulla and Tarutung pull-apart basins.
- The Angkola Fault Zone from Padangsidempuan northwards becomes broken into smaller segments and exhibit more dominant extensional/normal faulting component approaching the Sarulla pull-apart basin.

Analysis on geological slip rates of the Renun and Sianok Fault segments shows that slip rates of both ends of the major fault bifurcation are identical, which is about ~14 mm/yr. Thus, total slip rates across the Toru and Angkola Fault

Zones should also be about 14 mm/yr. The slip rate on Toru segment is 9.3 ± 1.8 mm/yr.; hence the slip rate on Angkola is about 4 - 5 mm/yr. However, further study is encouraged to measure the slip rate on Angkola Fault directly.

Field observations strongly suggests that (at least part of) Toru Fault segment is creeping. In other word, it moves continuously on the order of several millimetres per year. This is the first actual evidence of fault creeping along the Sumatran Fault Zone. Hence, it is necessary to investigate further this aspect by conducting detailed paleoseismological investigations in order to evaluate how much of fault movement is being accommodated by creeping, or whether there are still significant amount of movement is being accommodated by stick-slip mechanisms, therefore still capable of generating large earthquakes.

ACKNOWLEDGMENTS

The author thanks Dr. Didiek Djawardi and PT. North Sumatra Hydro Energy for facilitating this study and providing LIDAR data for the Toru River area. The author is also grateful to the helps of the field team, especially Dr. Mudrik R. Daryono and Mr. Bambang W. Suwargadi. This work is supported by PT. North Sumatra Hydro Energy and Puslit Geoteknologi LIPI.

REFERENCES

- Alloway, B.V., Pribadi, A., Westgate, J.A., Bird, M., Fifield, L.K., Hogg, A., and Smith, I., 2004. Correspondence between glass-FT and 14C ages of silicic pyroclastic flow deposits sourced from Maninjau caldera, west-central Sumatra. *Earth and Planetary Science Letters*, 227, p.121-133. DOI: 10.1016/j.epsl.2004.08.014
- Aspden, J.A., Kartawa, W., Aldiss, D.T., Djunuddin, A., Whandoyo, R., Diatma, D., Clarke, M.C.G., and Harahap, H. 1982. *The Geology of the Padangsidempuan and Sibolga Quadrangle, Sumatra*. Geological Research and Development Centre.
- Bakun, W.H. and Lindh, A.G., 1985. The Parkfield, California, earthquake prediction experiment. *Science*, 229 (4714), p.619-624. DOI: 10.1126/science.229.4714.619
- Bakun, W.H. and McEvilly, T.V., 1984. Recurrence models and Parkfield, California, earthquakes. *Journal of Geophysical Research*, 89 (B5), p.3051-3058. DOI: 10.1029/JB089iB05p03051
- Becker, J., Saunders, W., and van Dissen, R., 2005. Planning for The Development of Land on or close to Active Faults: A study of the adoption and use of the Active Fault Guidelines. *Internal Report*, GNS New Zealand, Lower Hutt (Unpublished).
- Bellier, O., Sebrier, M., Pramumidjojo, S., Beaudouin, Th., Harjono, H., Bahar, I., and Forni, O., 1997. Paleoseismicity and seismic hazard along the Great Sumatran fault (Indonesia). *Journal Geodynamics*, 24 (1-4), p.169-183. DOI: 10.1016/S0264-3707(96)00051-8
- Ben-Zion, Y. and Malin, P., 1993. Interaction of the San Andreas fault creeping segment with adjacent great rupture zones and earthquake recurrence at Parkfield. *Journal of Geophysical Research*, 98 (B2), p.2135-2144. DOI: 10.1029/92JB02154
- Bradley, K.E., Feng, L., Hill, E.M., Natawidjaja, D.H., and Sieh, K., 2017. Implications of the diffuse deformations of the Indian Ocean lithosphere for slip partitioning of oblique plate convergence in Sumatra. *Journal of Geophysical Research Solid Earth*, 122 (1), p.572-591. DOI: 10.1002/2016JB013549.
- Chesner, C.A., Rose, W.I., Deino, A., Drake, R., and Westgate, J.A., 1991. Eruptive history of Earth's largest Quaternary caldera (Toba, Indonesia) clarified. *Geology*, 19 (3), p.200-203. DOI: 10.1130/0091-7613(1991)019<0200:EHOESL>2.3.CO;2
- Curry, J.R., 2005. Tectonics and history of the Andaman Sea region. *Journal of Asian Earth Sciences*, 25 (1). p.187-232. DOI: 10.1016/j.jseaes.2004.09.001

- Curry, J.R., Moore, D., Lawver, L., Emmel, G.F., Raitt, R., Henry, M., and Kieckhefer, R., 1979. Tectonics of the Andaman Sea and Burma. *American Association of Petroleum Geologists Memoir*, 29, p.189-198.
- Daryono, M.R., Natawidjaja, D.H., and Sieh, K., 2012. Twin-surface ruptures of the March 2007>6 earthquake doublet on the Sumatran fault. *Bulletin of The Seismological Society of America*, 102 (6), p.2356-2367. DOI: 10.1785/0120110220
- Diament, M., Harjono, H., Karta, K., Deplus, C., Dahrin, D., Zen Jr., M.T., Gerard, M., Lassal, O., Martin, A., and Malod, J., 1992. Mentawai fault zone off sumatra - a new key to the geodynamics of western Indonesia. *Geology*, 20 (3), p.259-262. DOI: 10.1130/0091-7613(1992)020<0259:MFZOSA>2.3.CO;2
- Engdahl, E.R., Villasenor, A., DeShon, H.R., and Thurber, C.H., 2007. Teleseismic relocation and assesment of seismicity (1918 - 2005) in the region of the 2004 Mw 9.0 Sumatra-Andaman and the 2005 Mw 8.6 Nias Island great earthquakes. *Bulletin of The Seismological Society of America*, 97 (1A), S43-S61. DOI: 10.1785/0120050614
- Fitch, T., 1972. Plate convergence, transcurrent faults, and internal deformation adjacent to southeast Asia and the western Pacific. *Journal of Geophysical Research*, 77 (23), p.4432-4462. DOI: 10.1029/JB077i023p04432
- Genrich, J.F., Bock, Y., and McCaffrey, R., 2000. Distribution of slip at the northern Sumatran fault system. *Journal of Geophysical Research*, 105 (B12), p.28,327-28,41. DOI: 10.1029/2000JB900158
- Gunderson, R.P., Dobson, P.F., and Sharp, W.D., 1995. Geology and thermal features of the sarulla contract block, north Sumatra, Indonesia. *Proceedings of The World Geothermal Congress*. Japan, p. 687-692.
- Gunderson, R.P., Ganefianto, N., and Riedel, K., 2000. Exploration results in the Sarulla block, north Sumatra, Indonesia. *Proceedings of the World Geothermal Congress*, Japan, p.1183-1188.
- Hickman, R.G., Dobson, P.F., van Gerven, M., Sagala, B.B., and Gunderson, R.P., 2004. Tectonic and straiographic evolution of the Sarulla graben geothermal area, North Sumatra, Indonesia. *Journal of Asian Earth Sciences*, 23 (3), p.435-448. DOI: 10.1016/S1367-9120(03)00155-X
- Huchon, P., and Le Pichon, X., 1984. Sunda Strait and Central Sumatra fault. *Geology*, 12 (11), p.668-672. DOI: 10.1130/0091-7613(1984)12<668:SSACSF>2.0.CO;2
- Hurukawa, N., Wulandari, B.R., and Kasahara, M., 2014. Earthquake history of the Sumatran Fault, Indonesia, since 1892, derived from rlocation of large earthquake. *Bulletin of The Seismological Society of America*, 104 (4). DOI: 10.1785/0120130201
- Katili, J.A. and Hehuwat, F., 1967. On the occurrence of large transcurrent faults in Sumatra, Indonesia. *Journal of Geoscience*, Osaka City University, 10, p.5-17.
- Kerr, J., Nathan, S., van Dissen, R., Webb, P., Brunson, D., and King, A., 2003. *Planning for Development of Land on or Close to Active Faults: A guideline to assist resource management planners in New Zealand*. edited by Science, Geological and Nuclear: Ministry for The Environment, 67pp.
- Darren F.M., Petraglia, M., Smith, V.C., Morgan, L.E., Barfod, D.N., Ellis, B.S., Pearce, N.J., Pal, J.N., and Korisettarf, R., 2014. A high-precision 40 Ar/39 Ar age for the Young Toba Tuff and dating of ultra-distal tephra: forcing of Quaternary climate and implications for hominin occupation of India. *Quaternary Geochronology*, 21, p.90-103. DOI: 10.1016/j.quageo.2012.12.004
- McCaffrey, R., 1991. Slip vectors and stretching of the Sumatran fore arc. *Geology*, 19 (9), p.881-884. DOI: 10.1130/0091-7613(1991)019<0881:SVASOT>2.3.CO;2
- McClymont, B., 2001. Building on the edge - The use and Development of land on or close to Fault Lines. *Internal Report*, Parliamentary Commissioner for the Environment, Wellington New Zealand (Unpublished).

- Nalbant, S.S., Steacy, S., Sieh, K., Natawidjaja, D.H., and McCloskey, J., 2006. Seismology: Earthquake risk on the Sunda trench. *Nature*, 435, p.757-758. DOI: 10.1038/nature435756a
- Natawidjaja, D.H., 2012. Dekade teror gempa di Sumatra. *GEOMAGZ*, 1 (4).
- Natawidjaja, D.H., Sapiie, B., Darsono, M.R., and Marliyani, G.I., 2017. Geologi Gempa Indonesia. In: Irsyam, M., Natawidjaja, D.H., Meilano, I., and Widiyantoro, S., 2016. *Peta Sumber dan Bahaya Gempa Indonesia tahun*. Bandung: Kementrian PUPR
- Natawidjaja, D., Sieh, K., Ward, S., Edwards, R., Suwargadi, B., and Galetzka, J., 2001. Large active faults along the Sumatran plate margin and their seismic threat to Indonesia, Malaysia and Singapore. *Geosea-Indonesian Association of Geologist Geosea 2001*. Yogyakarta, Indonesia.
- Natawidjaja, D.H., Latief, H., Triyoso, W., and Suwargadi, B.W., 2007a. Crustal Deformations, Earthquake and Tsunami Hazards of the Sumatran Plate Margin. *Internal Report, RUTI - Kantor Menristek*, (Unpublished).
- Natawidjaja, D.H., 2003. *Neotectonics of the Sumatran Fault and paleogeodesy of the Sumatran subduction zone*.
- Natawidjaja, D.H., 2005. The Past, recent, and future giant earthquakes of the Sumatran megathrust. In: JASS05 Great Earthquakes in the Plate Subduction. Nagoya, Japan: Nagoya University and the JSPS.
- Natawidjaja, D.H., Sieh, K., Galetzka, J., Suwargadi, B.W., Cheng, H., Edwards, R.L., and Chlieh, M., 2007b. Interseismic deformation above the Sunda megathrust recorded in coral microatolls of the Mentawai Islands, West Sumatra. *Journal of Geophysical Research*, 112 (B02404), p.1-27. DOI: 10.1029/2006JB004450
- Natawidjaja, D.H., Sieh, K., Chlieh, M., Galetzka, J., Suwargadi, B.W., Cheng, H., Edwards, R.L., Avouac, J.P., and Ward, S.N., 2006. Source Parameters of the great Sumatran megathrust earthquakes of 1797 and 1833 inferred from coral microatolls. *Journal of Geophysical Research* 111 (B06403), p.1-37. DOI: 10.1029/2005JB004025
- Natawidjaja, D.H., Sieh, K., Ward, S.N., Cheng, H., Edwards, R.L., Galetzka, J., and Suwargadi, B.W., 2004. Paleogeodetic records of seismic and aseismic subduction from central Sumatran microatolls, Indonesia. *Journal of Geophysical Research*, 109 (B4) (4306), p.1-34. DOI: 10.1029/2003JB002398
- Natawidjaja, D.H., 2017. Updating active fault map and slip rates along the Sumatran Fault Zone, Indonesia. In: *Global Qolloquium on Geoscience and Engineering LIPI 2017*, edited by Mukti, Jayakarta Hotel, Bandung: Puslit Geoteknologi LIPI.
- Natawidjaja, D.H. and Triyoso, W., 2007. The Sumatran Fault Zone: From source to hazards. *Journal of Earthquake and Tsunami*, 1 (1), p.21-47. DOI: 10.1142/S1793431107000031
- Ninkovitch, D., Shackleton, N.J., Abdel-Monem, A.A., Obradovich, J.D., and Izett, G., 1978. K-Ar age of the late Pleistocene eruption of Toba, north Sumatra. *Nature*, 276, p.574-577. DOI: 10.1038/276574a0
- Prawirodirdjo, L., Bock, Y., Genrich, J., Puntodewo, S.S.O., Rais, J., Subarya, C., and Sutisna, S., 1999. One century of tectonic deformation along the Sumatran Fault from triangulation and GPS surveys. *Journal of Geophysical Research*, 105 (B12), p.28,343-28,361. DOI: 10.1029/2000JB900150
- Sieh, K., Bock, Y., Edwards, L., Taylor, F., and Gans, P., 1994. Active tectonics of Sumatra. *Geological Society of America Bulletin*, 26, p.A-382.
- Sieh, K. and Natawidjaja, D.H., 2000. Neotectonics of the Sumatran fault, Indonesia. *Journal of Geophysical Research*, 105 (B12), p.28,295-28,326. DOI: 10.1029/2000JB900120
- Sieh, K., Natawidjaja, D.H., Meltzner, A. J., Shen, C.C., Cheng, H., Li, K.S., Suwargadi, B.W., Galetzka, J., Philiposian, B., and Edwards, R.L., 2008. Earthquake supercycles inferred from sea-level changes recorded in the corals of West Sumatra. *Science*, 322 (5908), p.1674-1678. DOI: 10.1126/science.1163589

Storey, M., Roberts, R.G., and Saidin, M., 2012. Astronomically calibrated $^{40}\text{Ar}/^{39}\text{Ar}$ age for the Toba super eruption and global synchronization of late Quaternary records. *PNAS*, 109 (46), p.18684-18688. DOI: 10.1073/pnas.1208178109

Weller, O., Lange, D., Tilmann, F., Natawidjaja, D.H., Rietbrock, A., Collings, R., Gregory,

L., 2012. The structure of the Sumatran fault revealed by local seismicity. *Geophysical Research Letters*, 39 (L01306). DOI: 10.1029/2011GL050440

Yeats, R.S., Sieh, K., and Allen, C.R., 1997. *The Geology of Earthquakes*. New York. Oxford University Press. DOI: 10.1086/515990

160